

**Youla S. Tsantrizos**  
Boehringer Ingelheim  
(Canada) Ltd.,  
Research and Development,  
2100 Cunard Street,  
Laval (Québec)  
Canada H7S 2G5

Received 2 June 2004;  
accepted 22 June 2004

Published online 3 September 2004 in Wiley InterScience (www.interscience.wiley.com). DOI 10.1002/bip.20127

---

## The Design of a Potent Inhibitor of the Hepatitis C Virus NS3 Protease: *BILN 2061* – From the NMR Tube to the Clinic

**Abstract:** The virally encoded serine protease NS3/NS4A is essential to the life cycle of the hepatitis C virus (HCV), an important human pathogen causing chronic hepatitis, cirrhosis of the liver, and hepatocellular carcinoma. Until very recently, the design of inhibitors for the HCV NS3 protease was limited to large peptidomimetic compounds with poor pharmacokinetic properties, making drug discovery an extremely challenging endeavor. In our quest for the discovery of a small-molecule lead that could block replication of the hepatitis C virus by binding to the HCV NS3 protease, the critical protein–polypeptide interactions between the virally encoded NS3 serine protease and its polyprotein substrate were investigated. Lead optimization of a substrate-based hexapeptide, guided by structural data, led to the understanding of the molecular dynamics and electronic effects that modulate the affinity of peptidomimetic ligands for the active site of this enzyme. Macrocyclic  $\beta$ -strand scaffolds were designed that allowed the discovery of potent, highly selective, and orally bioavailable compounds. These molecules were the first HCV NS3 protease inhibitors reported that inhibit replication of HCV subgenomic RNA in a cell-based replicon assay at low nanomolar concentrations. Optimization of their biopharmaceutical properties led to the discovery of the clinical candidate *BILN 2061*. Oral administration of *BILN 2061* to patients infected with the hepatitis C genotype 1 virus resulted in an impressive reduction of viral RNA levels, establishing proof-of-concept for HCV NS3 protease inhibitors as therapeutic agents in humans. © 2004 Wiley Periodicals, Inc. *Biopolymers (Pept Sci)* 76: 309–323, 2004

**Keywords:** hepatitis C (HCV); NS3 serine protease; macrocyclic peptides; clinical candidate *BILN 2061*; structure-based drug design; crystal structure of an HCV NS3-bound inhibitor; macrocyclic  $\beta$ -strand mimics

---

### INTRODUCTION

The alarming spread of hepatitis C viral (HCV) infections and the consequences associated with chronic hepatitis C has resulted in a worldwide severe medical problem. HCV was identified in the late eighties as the etiological agent of non-A and non-B hepatitis.<sup>1</sup> It

is currently estimated that more than 170 million people worldwide are infected with the HCV virus, transmitted mainly through contaminated blood.<sup>2</sup> In the majority of cases (>80%), the immune system is not capable of clearing the infection, which then becomes chronic. Following a relatively lengthy asymptomatic period (10–20 years), chronic infection usu-

---

Correspondence to: Youla S. Tsantrizos; email: ytsantrizos@lav.boehringer-ingelheim.com

*Biopolymers (Peptide Science)*, Vol. 76, 309–323 (2004)

© 2004 Wiley Periodicals, Inc.

ally progresses to end-stage liver diseases such as cirrhosis of the liver and hepatocellular carcinomas.<sup>3</sup> These conditions have become the leading indication for liver transplantations. An estimated 10,000 deaths occur annually in the United States alone that can be linked to complications arising from HCV infections.

Currently there are no vaccines that can prevent HCV infection in humans,<sup>4</sup> and options for therapy are limited to pegylated interferons (IFN- $\alpha$ )<sup>5</sup> administered intravenously in combination with the broad-spectrum antiviral nucleoside ribavirin.<sup>6</sup> However, the treatment is associated with severe side effects, and sustained reduction in viral load is achieved in only half of patients infected with HCV genotype 1, the most prevalent genotype in industrialized nations. There is an urgent need for new anti-HCV drugs that will address this worldwide medical problem.

The hepatitis C virus is a small enveloped virus with a positive single-stranded RNA genome that closely resembles other flaviviruses (e.g., yellow fever, dengue fever) and pestiviruses (e.g., bovine viral diarrhea virus). Recently, HCV was classified in a separate genus within this family, and is now referred to as a hepacivirus.<sup>7</sup> The viral genome of ~9600 nucleotides encodes a precursor polypeptide of approximately 3010 amino acids, which is processed both co- and posttranslationally to produce structural (C, E1, E2, p7) and nonstructural (NS2, NS3, NS4A, NS4B, NS5A, NS5B) proteins (Figure 1).<sup>8,9</sup> The virally encoded HCV nonstructural (NS) proteins NS2

(protease), NS3/NS4A (protease, helicase, and ATPase), and NS5B (RNA-dependent RNA polymerase) are attractive targets for antiviral therapy as their catalytic function is essential for in vivo viral replication.<sup>10</sup> Unfortunately, this seemingly simple virus is very difficult to defeat, and in spite of intensive efforts by researchers around the world, potential anti-HCV therapeutic agents are still in the early phases of preclinical or clinical development.<sup>11–13</sup> Complete elucidation of the HCV life cycle, and consequently, drug discovery, has been hampered by the inability to replicate the hepatitis C virus in cell culture. Recently, the development of a human hepatoma cell line (Huh-7 cells), which can efficiently replicate cloned subgenomic HCV RNA, provided a major advancement in the field.<sup>14,15</sup> This cell-based assay has become an indispensable tool in the evaluation of potential anti-HCV drug candidates. In addition, progress has been made in the development of HCV-infected animal models, including the recently validated infected chimpanzee model (the only animal species known to sustain HCV replication)<sup>16,17</sup> and a chimeric mouse model harboring transplanted human hepatocytes that can be inoculated with serum from HCV-infected patients.<sup>18</sup>

The macrocyclic  $\beta$ -strand mimic **BILN 2061 (2)** is the first inhibitor of the HCV NS3/NS4A serine protease reported with proven antiviral effects in humans (Scheme 1).<sup>19,20</sup> Since this compound is the first of its class to enter clinical development, it provided clini-

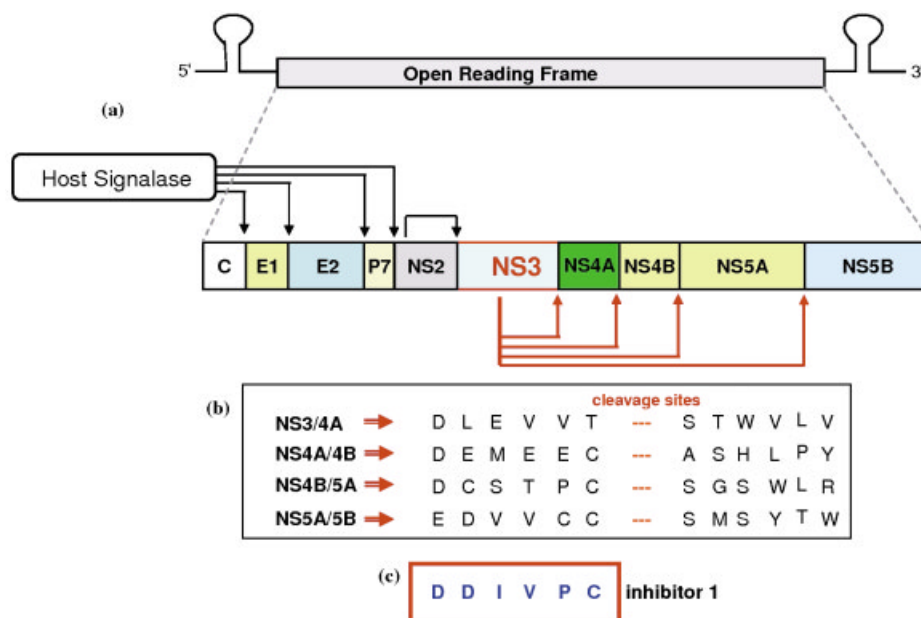
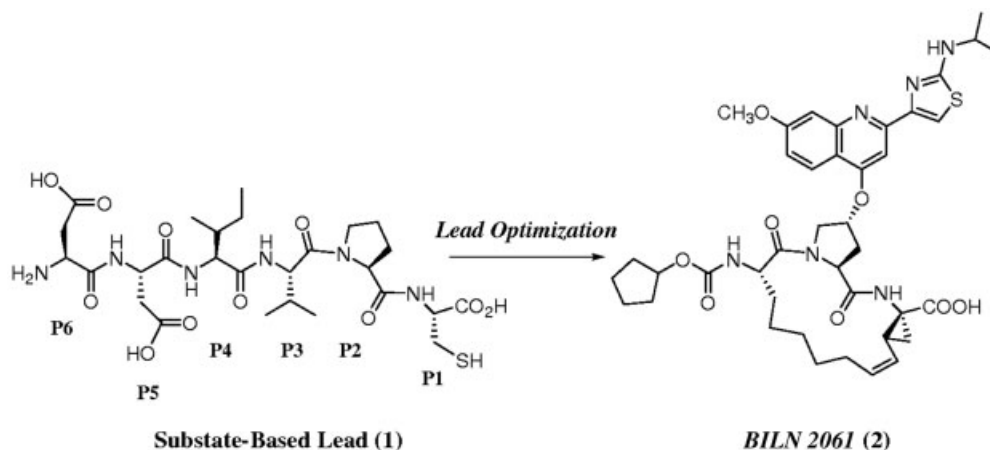


**FIGURE 1** (a) Polyprotein translation product of the HCV ~9.6 kilobase (+) RNA genome; (b) substrate specificity of NS3 protease at the four cleavage sites of the NS region; (c) substrate-based initial lead structure (1) of a competitive inhibitor of the NS3 protease.



**SCHEME 1** Design of **BILN 2061**, a clinically useful HCV NS3 protease inhibitor from a substrate-based hexapeptide.

cal validation for its target enzyme and real hope for the current and future approaches to HCV chemotherapy.<sup>21</sup> This report is a brief summary of the drug discovery efforts at Boehringer-Ingelheim (Canada) Ltd. that led to the discovery of **BILN 2061 (2)**, starting from the substrate-based lead hexapeptide **1** (Scheme 1). Some of the critical structural studies that guided the design of the  $\beta$ -strand backbone scaffold of **2**, mimicking the NS3-bound conformation of **1**, is presented. The structure–activity relationship (SAR) of this novel class of inhibitors is also described. The results of this investigation highlight the staying power of structure-based, rational drug design and the role of peptide research in medicinal chemistry. Furthermore, this review is a unique example of the enormous value of peptide mimics that can efficiently disrupt interactions between large biomolecules relevant to biological targets in medical interventions.

### THE HCV NS3/NS4A SERINE PROTEASE—STRUCTURE AND FUNCTION

Proteolytic processing of the HCV ~3010 amino acid polyprotein is essential for release of at least 10 mature viral proteins: HO<sub>2</sub>C–C–E1–E2–p7–NS2–NS3–NS4A–NS4B–NS5A–NS5B–NH<sub>2</sub> (Figure 1). The nucleocapsid protein C,<sup>22</sup> two virion glycoproteins E1 and E2, and the p7 protein (of yet unknown function) are released from the polyprotein through the action of host signal peptidases.<sup>23</sup> However, the two virally encoded proteases, NS2 and NS3, are responsible for processing the entire nonstructural region (NS2  $\Rightarrow$  NS5B) of the HCV polyprotein (Figure 1). The NS2

to NS5B proteins inclusively are thought to comprise the nonstructural proteins involved in replication and polyprotein processing.<sup>24</sup> The cleavage between NS2 and NS3 is performed in an autoproteolytic manner by the NS2/NS3 protease, whereas proteolytic processing of the remaining polyprotein (NS3  $\Rightarrow$  NS5B) is catalyzed by the N-terminal domain of the NS3 (~180 amino acid residues) which harbors a chymotrypsin-like serine protease.<sup>27,28</sup> Given the indispensable role of the latter enzyme in the maturation process of the HCV polyprotein, and consequently, HCV infectivity, it is not surprising that it has been a prime target for antiviral therapy.

The NS3 67 kDa protein is a multifunctional enzyme that in addition to its N-terminal protease domain, has a C-terminal domain (~460 amino acid residues) that harbors RNA-dependent helicase and ATPase catalytic properties.<sup>29</sup> X-ray crystallography of the full-length NS3 has revealed that the protease and helicase/ATPase domains are segregated and connected by a single strand (Figure 2a).<sup>30</sup> This structural segregation is consistent with *in vitro* investigations demonstrating that each separated domain retains its respective catalytic function.<sup>29</sup> However, the catalytic efficiency of each domain is modulated by the presence of the other and, *in vivo*, possibly by the presence of other viral and host proteins. The NS3 protease–helicase interdomain cross-talk has been supported by a number of observations. For example, with the full-length NS3, an enhancement of protease activity (~5-fold) was observed in the presence of a uridine oligomer [poly(U)], which was not observed with the isolated protease domain.<sup>31</sup> This data suggested that binding of the poly(U) to the helicase domain (or possibly both domains<sup>32</sup>) stimulated pro-

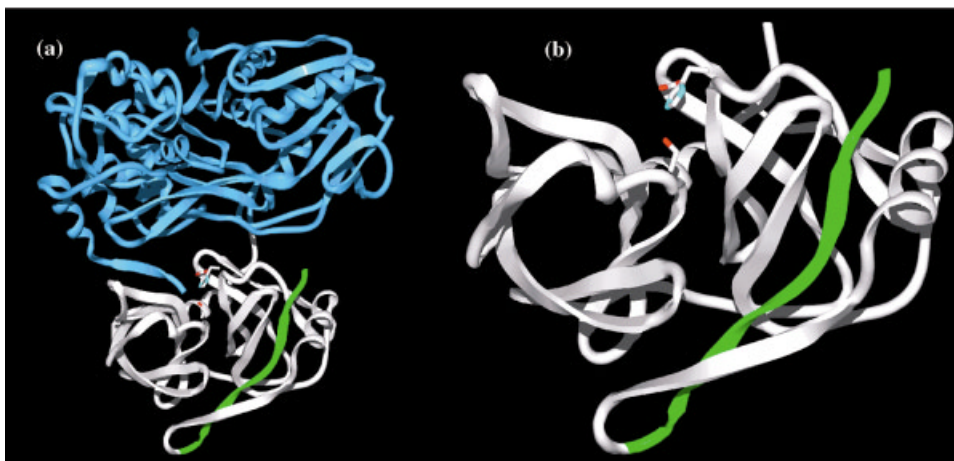


**FIGURE 2** (a) Full-length NS3/NS4A (protease domain in grey, helicase/ATPase in blue, NS4A in green); (b) NS3/NS4A protease domain alone (catalytic residues highlighted in ball-and-stick).

tease activity. Interestingly, concentration-dependent inhibition of the helicase activity by the NS4A (the NS3 cofactor) was also observed,<sup>32</sup> further indicating that the two catalytic sites of the NS3 modulated the activity of one another through some yet unclear allosteric mechanism.<sup>33</sup>

The NS3 protease domain is fairly unique among serine proteases in that it is activated by its structure-modifying cofactor NS4A (Figure 2b).<sup>30,32</sup> Interactions between the NS3 and the 54 amino acids of NS4A (in 1:1 ratio) induce conformational changes that significantly reduce (but not entirely eliminate) the plasticity of the NS3 protease. The interaction between the NS3 protease domain and the NS4A requires the 22 N-terminal residues of the protease and the central 12 residues of the NS4A. Therefore, for *in vitro* assays (or X-ray crystallography), the cofactor can also be supplied as a synthetic 12-residue peptide (NS4A<sub>peptide</sub>) without significant loss of activation of the NS3 protease. Crystallographic evidence of the NS3 protease alone (in the absence of the NS4A) has revealed a chymotrypsin-like overall structure, where the active site residues (Asp 81, His 57, and Ser 139), and especially the N-terminal residues of the protease, are loosely structured.<sup>34</sup> However, in the presence of the NS4A (or its essential fragment NS4A<sub>peptide</sub>),<sup>30,35,36</sup> the N-terminal subdomain of the protease forms an eight-stranded  $\beta$ -barrel, where one strand is contributed by the NS4A, as an integral part of the NS3/NS4A protease complex (Figure 2b). The active site of the HCV NS3 serine protease lies in the shallow and solvent-exposed cleft between the two  $\beta$ -barrels. Two of its catalytic residues (His 57 and Asp 81) are located in the N-terminal subdomain and the third catalytic residue (Ser 139) is on the C-terminal subdomain (Figure 2b).

## LEAD OPTIMIZATION OF A SUBSTATE-BASED HEXAPEPTIDE

The first insight into the design of peptidomimetic inhibitors of the HCV NS3 protease came from the observation that N-terminal proteolysis products of substrates corresponding to the *trans* sites (Figure 1), but not the *cis* site, of NS3/NS4A can act as inhibitors of the NS3 protease.<sup>37,38</sup> Initial SAR revealed that optimal binding of a hexapeptide ligand required acidic anchors at both ends of the molecule (corresponding to the P1  $\Rightarrow$  P6 of the N-terminal product of a dodecapeptide substrate; for protease subsite nomenclature, see Ref. 39) and that for optimum *in vitro* potency, cysteine was the preferred residue at P1 (Scheme 1). Examples of these weak inhibitors include the N-acetyl derivative of hexapeptide **1**, AcNH-DDIVPC-CO<sub>2</sub>H (compound **3**, Figure 3)<sup>37</sup> and AcNH-DEMEEC-CO<sub>2</sub>H,<sup>38</sup> the latter peptide corresponding to the NS4A/NS4B cleavage site (Fig. 1b). Interestingly, replacement of the C-terminal carboxylic acid moiety (P1) with an activated carbonyl moiety did not produce a substantial increase in the potency of these peptides; however, these analogs appeared less selective for their intended target than the corresponding carboxylic acid derivatives.<sup>11</sup>

In the course of *lead optimization*, automated high-throughput parallel synthesis was used to synthesize libraries of novel compounds having substitutions at every position of the lead hexapeptide **3** (Figure 3). These investigations led to the identification of P1 replacements, such as *n*-propyl and cyclopropyl glycine derivatives, which provided chemically more stable inhibitors (e.g., hexapeptides **4** and **5**, respectively) than the initial cysteine analog **3** with reasonable potency.<sup>40,41</sup> *In vitro* evaluation of derivatives **4**



theless, truncation of hexapeptide **7** to the corresponding tetrapeptide **8** resulted in a significant decrease in intrinsic potency (Figure 3). Insight into this apparent contradiction was provided by Steinköhler and co-workers, who examined the role of the P5 and P6 residues using pre-steady-state kinetics.<sup>46</sup> Based on their observations, they proposed that the electrostatic surface potential of these residues enhances the collision rates between the peptidic ligand and the active site of NS3 protease.<sup>46</sup>

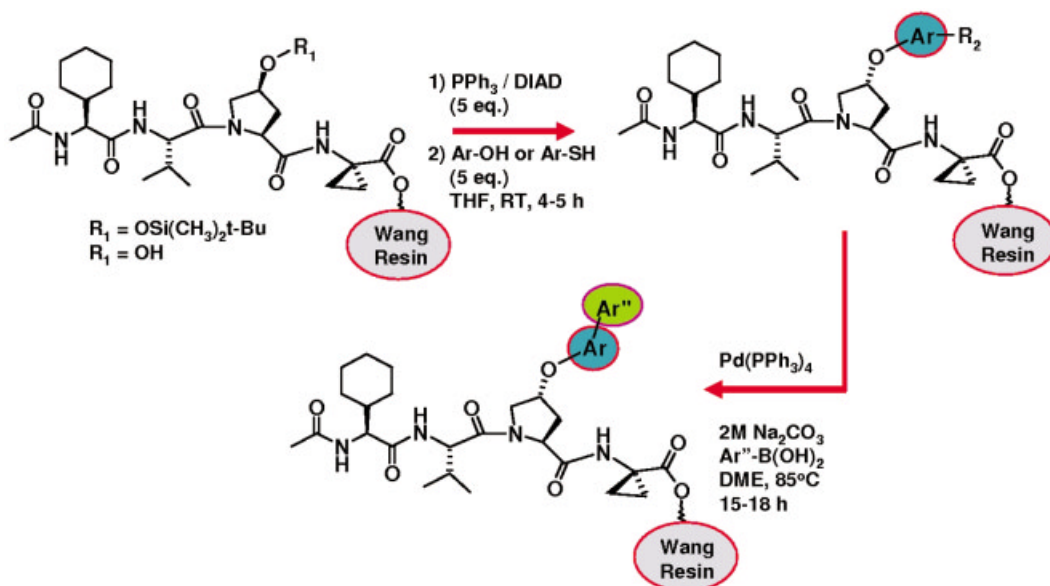
### SOLID-PHASE SYNTHESIS OF TETRAPEPTIDE LIBRARIES—OPTIMIZATION OF THE DIPOLE/QUADRUPOLE AND $\pi$ -STACKING LIGAND-NS3 INTERACTIONS

From the beginning of our HCV NS3 protease drug discovery program, automated solid-phase synthesis of peptide libraries permitted rapid evaluation of the SAR and the discovery of novel peptidomimetic inhibitors of the NS3 protease. Key compounds within these libraries were designed as structural probes for NMR and computational studies. In order to achieve broad structural diversity, numerous synthetic methodologies were adapted to solid-phase peptide chemistry, including cross-coupling reactions between polymer-bound peptides and commercially available building blocks under Mitsunobu<sup>47</sup> and Suzuki conditions.<sup>48</sup> A variety of aryl, biaryl, and heteroaryl reagents were attached to the 4-hy-

droxyproline moiety of P2 under Mitsunobu and Suzuki conditions; the overall synthetic methodology is shown in Scheme 2.<sup>49</sup> Consistent with our previous observations (Figure 3), further optimization of the P2 aromatic system resulted in a dramatic increase of the binding affinity of tetrapeptide ligands for the HCV NS3 protease.<sup>49</sup> Furthermore, these ligands were used to explore the NS3-bound conformation of the P2 moiety by NMR,<sup>50</sup> and the dipole/quadrupole/ $\pi$ -stacking interactions between the aromatic substituent and the NS3 binding pocket with molecular modeling calculations.<sup>49</sup>

In the absence of any NMR or X-ray data revealing the binding interactions between the aromatic substituent of the 4-hydroxyproline moiety and the NS3 protease, the main goal of the Mitsunobu and Suzuki libraries was to provide means by which we could probe the features of the NS3 binding pocket. A variety of building blocks, bearing electron-donating or electron-withdrawing groups, were specifically chosen in order to modulate the size and electrostatic potential of the aromatic system. An interesting trend in the intrinsic potency of the tetrapeptide ligands was observed (Figure 5), which correlated with the calculated electrostatic potentials of their P2 aromatic systems (Figure 4a). For example, tetrapeptide **16** was approximately 7-fold more potent than the unsubstituted quinoline analog **12** and approximately 130-fold more potent than the tetrapeptide **17** (Figure 5), consistent with the general trend of decreasing electrostatic potential in their corresponding quinolines (Figure 4a).

Based on NMR studies, the NS3-bound conformation of biaryl analogs (e.g., an analog of **14** shown in



SCHEME 2 Library synthesis on solid support.

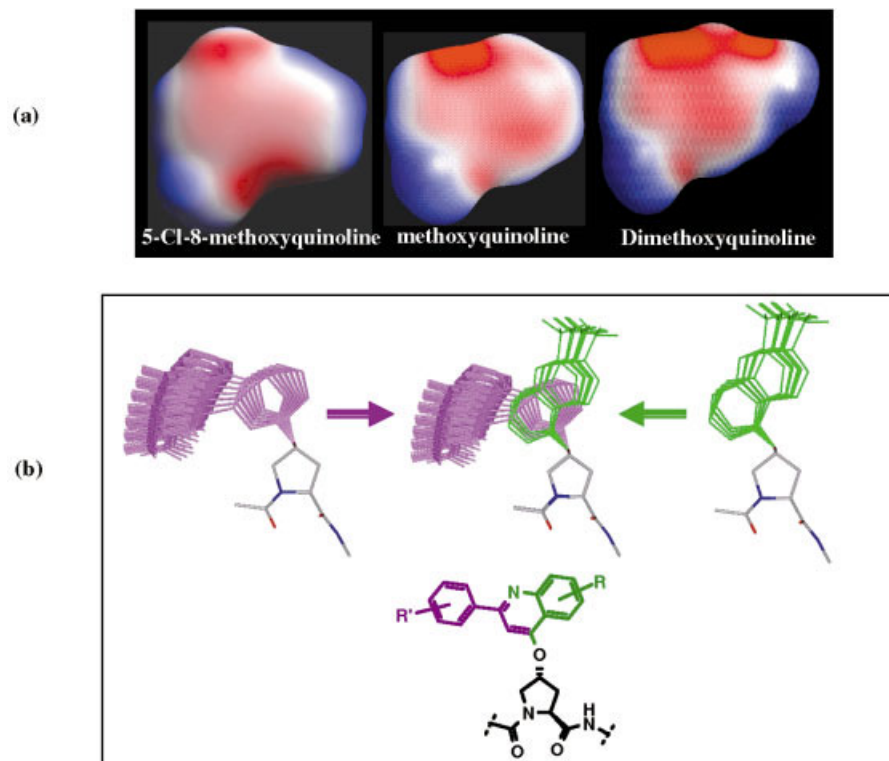


**FIGURE 4** SAR optimization guided by molecular modeling and NMR. (a) Electrostatic potential (ESP) of quinolines (model compounds of tetrapeptides **17**, **12** and **16**, respectively; red is negative ESP, blue is positive ESP); (b) NS3-bound conformation of the P2 aromatic moiety of the tetrapeptide inhibitors **14** and **15**.

purple; Figure 4b) was found to be significantly different from that of the quinoline analogs (e.g., compound **15** shown in green; Figure 4b), suggesting that the P2 binding pocket could accommodate hybrid tricyclic quinoline analogs, such as the 7-phenyl-4-hydroxyquinoline derivative **18**.<sup>50</sup> These cumulative SAR and structural/computational observations led to further optimization of the tetrapeptide inhibitors; as predicted by the electrostatic potential calculations and the NMR studies, compounds **16** and **18** were both approximately 7- to 10-fold more potent than the unsubstituted quinoline analog **12** (Figure 5). Furthermore, the observed SAR strongly suggested that in addition to the hydrophobic interactions, a dipole/quadrupole interaction between the aromatic system at the P2 moiety and the binding pocket of the NS3 protease was contributing to the affinity of the inhibitors for the enzyme.<sup>51</sup> This hypothesis was later confirmed by X-ray crystallography.<sup>52</sup>

The peptidic backbone of the quinoline derivatives (Figure 5) was expected to be more rigid than the earlier benzyloxy or naphthylmethoxy analogs (Figure 3). Surprisingly, the simultaneous optimization of both P1 and P2, with the (1*R*,2*S*)-vinyl ami-

nocyclopropane carboxylic acid (vinyl ACCA)<sup>53</sup> residue at P1 and a quinoline or methoxy quinoline at P2, resulted in greater increase of potency than what would have been expected based on the SAR of the corresponding naphthylmethoxy derivatives (some representative examples are shown in Figure 6). Unfortunately, in spite of the dramatically improved in vitro enzymatic potency of these tetrapeptides (i.e., ~21,000-fold increase in potency from hexapeptide **3** to tetrapeptide **23**, Figure 7), cell-based potency could not be observed in the replicon assay, even at the highest concentrations that they could be tested ( $EC_{50} > 5 \mu M$ , Figure 7), once again revealing the inherently poor biopharmaceutical properties of molecules with a highly peptidic nature.

#### DESIGN OF A MACROCYCLIC SCAFFOLD MIMICKING THE $\beta$ -STRAND NS3-BOUND CONFORMATION OF SUBSTRATE-BASED HEXAPEPTIDES

Based on the poor biopharmaceutical profile of compounds such as **23**, the need for a less peptidic scaffold

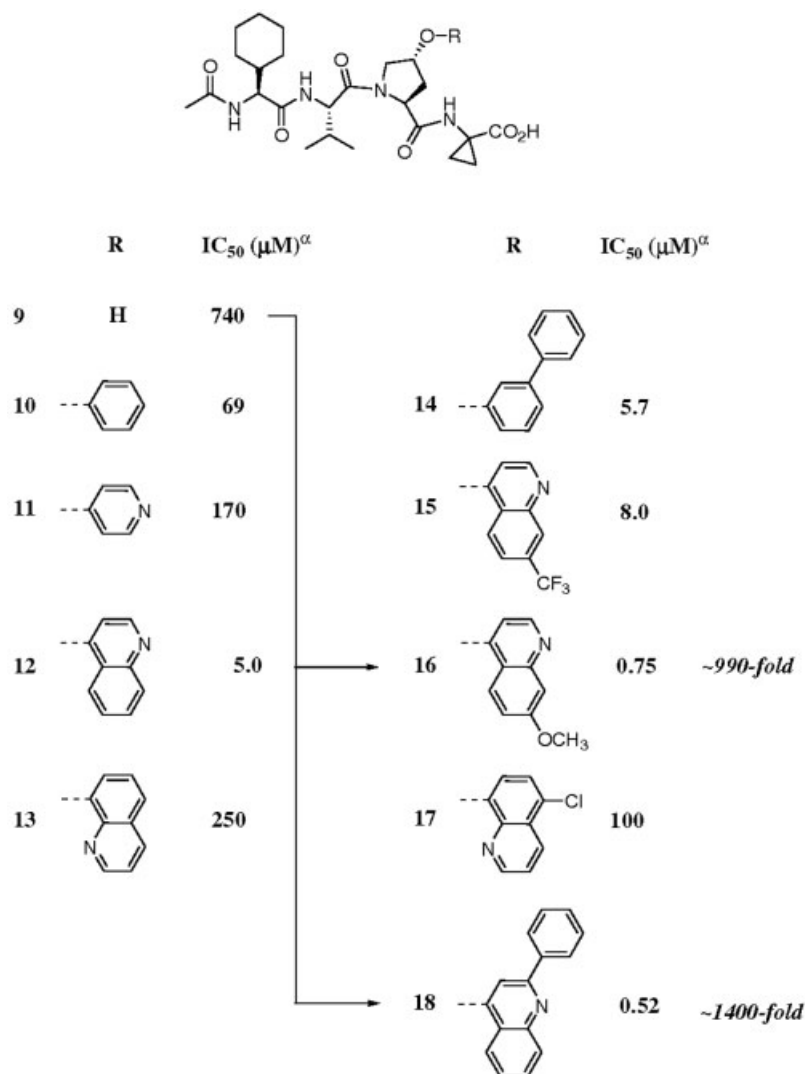
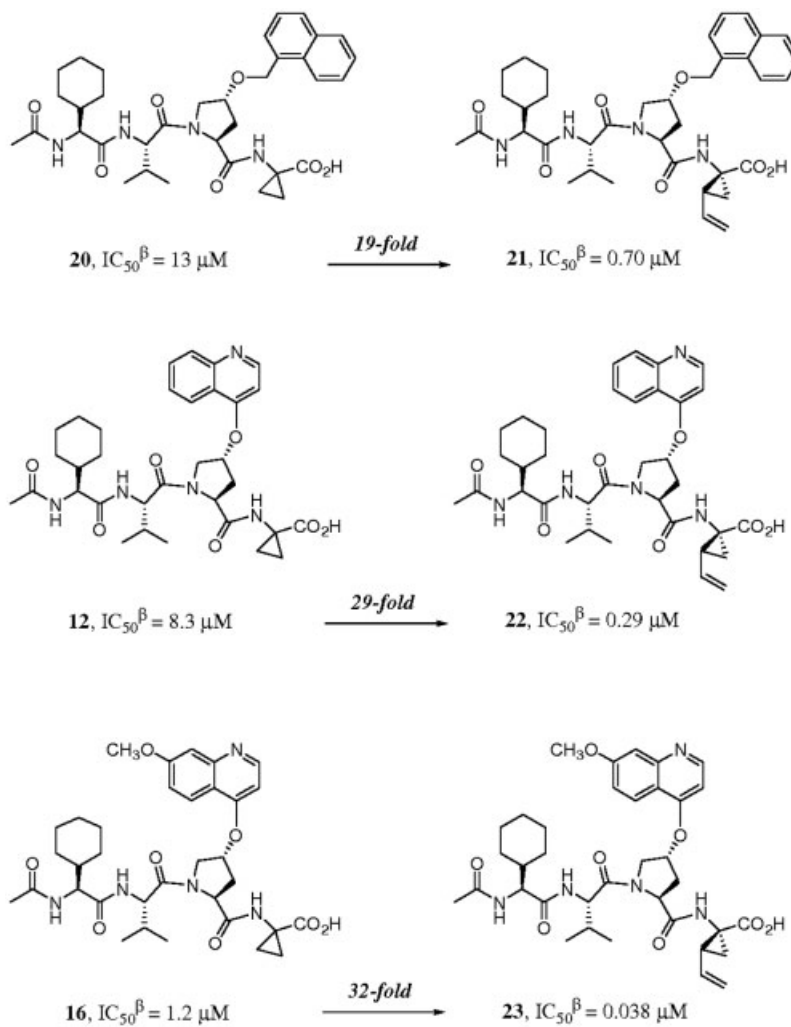


FIGURE 5 P2 Optimization of tetrapeptides.

fold than that of the linear tetrapeptides was clearly evident. Therefore, the bimolecular recognition elements involved in an NS3–ligand complex were further investigated. The interactions of the NS3 protease domain with the substrate-based hexapeptide **6** were previously explored by NMR and molecular modeling (Figure 8a).<sup>43,44</sup> As mentioned previously, these studies suggested that the main interactions between the hexapeptide and the enzyme involved the P1–P3 residues, binding in an extended,  $\beta$ -strand conformation.<sup>43</sup> Furthermore, in the inhibitor–protein complex, the P3 side chain was shown to be solvent exposed and in close proximity to the P1 *n*-propyl (norvaline) side chain. The P1 *n*-propyl side chain was folded inside the NS3 S1 binding pocket, placing the  $\delta\text{CH}_3$  in close proximity to the  $\alpha\text{H}$  of the P1 and the  $\gamma\text{CH}_3$  of the P3 valine residue (Figure 8a). Additional NMR

studies with tetrapeptides, having an ACCA residue at P1,<sup>54</sup> confirmed that the backbone of the shorter ligands was also adopting the extended  $\beta$ -strand conformation upon binding to the NS3. The structural differences between the free (in solution) and the NS3-bound state of these ligands were further explored by both NMR and computational studies.<sup>55</sup> Based on these studies, we concluded that the NH–C $\alpha$  bond of the P1 residue, in a free ligand, had to undergo a rotation of approximately 180° in order to adopt its NS3-bound conformation.<sup>55</sup> Therefore, the entropic penalty associated with the overall realignment of a ligand, into the preferred enzyme-bound conformation, was expected to have a negative impact on its binding energy. Hence, we embarked on the design of a rigid scaffold that could restrain the orientation of the P1 carboxylate anion to that of the



**FIGURE 6** Simultaneous optimization of the P1 and P2 residues.

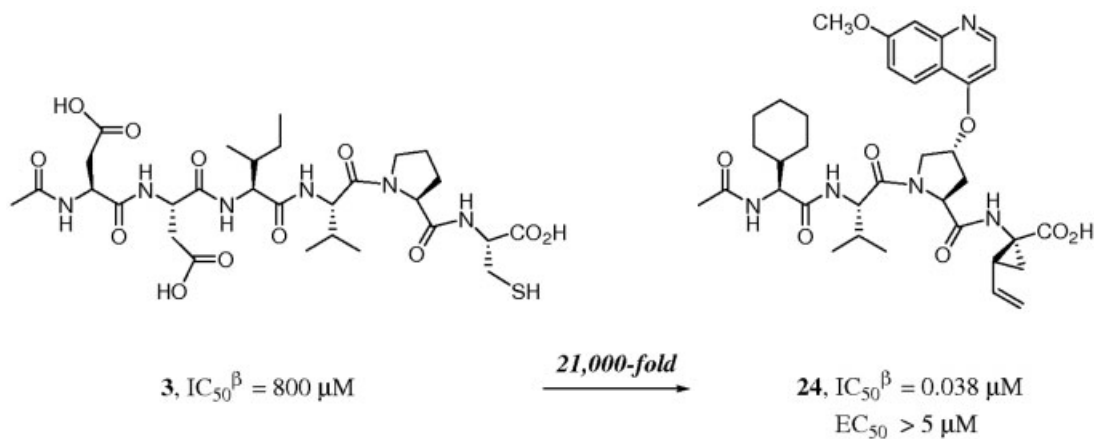


**FIGURE 7** Lead optimization: from hexapeptides to tetrapeptides.

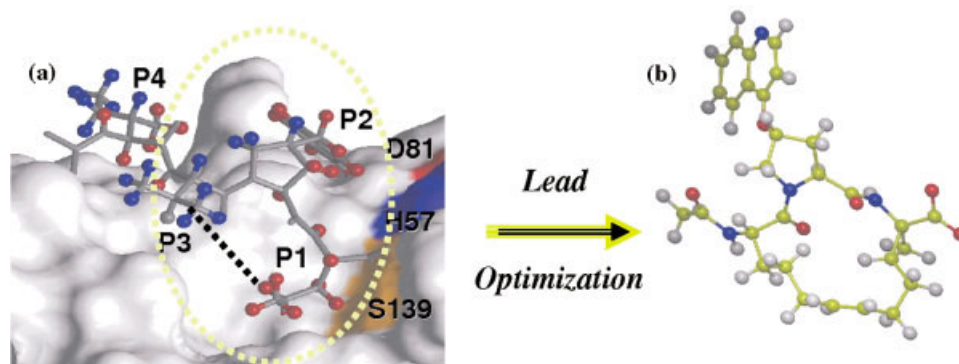


**FIGURE 8** (a) A model of hexapeptide 3 bound to the active site of the apo NS3 protease, created by docking the NMR-derived bound conformation of the hexapeptide (protons in blue indicate negative differential line broadening; protons in red indicate positive differential line broadening). (b) NMR-derived conformation of a 15-member ring macrocyclic inhibitor (an analog of compound **28** without the methoxy group).

NS3-bound orientation and simultaneously preorganize the peptidic backbone exclusively to an all-*trans* geometry ( $\beta$ -strand); the latter is a significant problem with proline-containing linear peptides, which usually exist as mixtures of *cis* and *trans* rotamers. We predicted that covalent linking of the P1–P3 side chains, creating a 14- to 16-member ring structure, could result in a peptidomimetic scaffold which in the *free state* would adopt the desired  $\beta$ -strand NS3-bound conformation; this assumption was later proven correct based on NMR studies (Figure 8b).<sup>55</sup> This rigid macrocyclic ligand was expected to pay a much lower entropic penalty for binding to the protease and, consequently, have a higher affinity for the enzyme than its corresponding acyclic precursor.<sup>52,56</sup>

## MACROCYCLIC INHIBITORS OF THE HCV NS3/NS4A PROTEASE

The design of rigid macrocyclic inhibitors began with an evaluation of the peptidic backbone of the previously developed tetrapeptide inhibitors, typified by compound **25** (Figure 9).<sup>52</sup> During these studies, we observed that the tetrapeptide scaffold **25**, as well as its truncated analog *N*-Boc derivative **26**, were void of any potency in our *in vitro* assay using the full-length HCV NS3/NS4A heterodimer (Figure 9).<sup>52</sup> However, we discovered that the 15-membered ring macrocyclic peptide **27** (with a double bond of the *Z* configuration) was a weak inhibitor.<sup>52</sup> Optimization of **27** by substitution of the proline with a 4-hydroxy-7-methoxyquinoline moiety,<sup>49</sup> as previously described, led to inhibitor **28** with an approximate 16,600-fold increase in potency over the “naked” scaffold **27**

(Figure 9) and approximate 50-fold and 2-fold increase in potency over the linear tetrapeptides **16** and **23**, respectively, (Figure 6). More importantly, the macrocyclic inhibitor **28** exhibited measurable cell-based potency (albeit low) in the replicon assay (Figure 9). Further optimization of the P2 quinoline substituent to the 2-phenyl-4-hydroxy-7-methoxy analog **29** led to an increase in intrinsic and cell-based potency by 2-fold and 16-fold, respectively, thus exhibiting a potency profile presumed acceptable of a potential preclinical candidate (Figure 9). As expected, a drop in enzymatic potency of approximately 36-fold was observed upon *cleaving* of the P1–P3 hydrocarbon linker to produce the corresponding open-chain analog **30** (Figure 9), thereby confirming the importance of macrocyclization.

Predictably, the binding affinity and potency of these inhibitors was highly dependent on the ring size and the stereochemistry of each chiral center.<sup>57</sup> For example, compound **29** was 180-fold more potent than its epimer **31**, further validating the specificity of these inhibitors for their intended molecular target. Steady-state kinetic analysis of the mode of inhibition of compound **29** demonstrated competitive inhibition of the NS3-NS4A protease heterodimer of genotype 1b with a  $K_i$  of 1.0 nM.<sup>52</sup> Inhibition of the HCV NS3-NS4A protease heterodimer of genotype 1a was also evaluated with the same inhibitor (compound **29**), demonstrating competitive inhibition with a  $K_i$  of 1.4 nM. These compounds were also found to be highly selective in inhibiting the HCV NS3 protease without inhibiting mammalian proteases, such as human leukocyte elastase and liver cathepsin B, even at concentrations exceeding 30  $\mu$ M.<sup>52</sup>

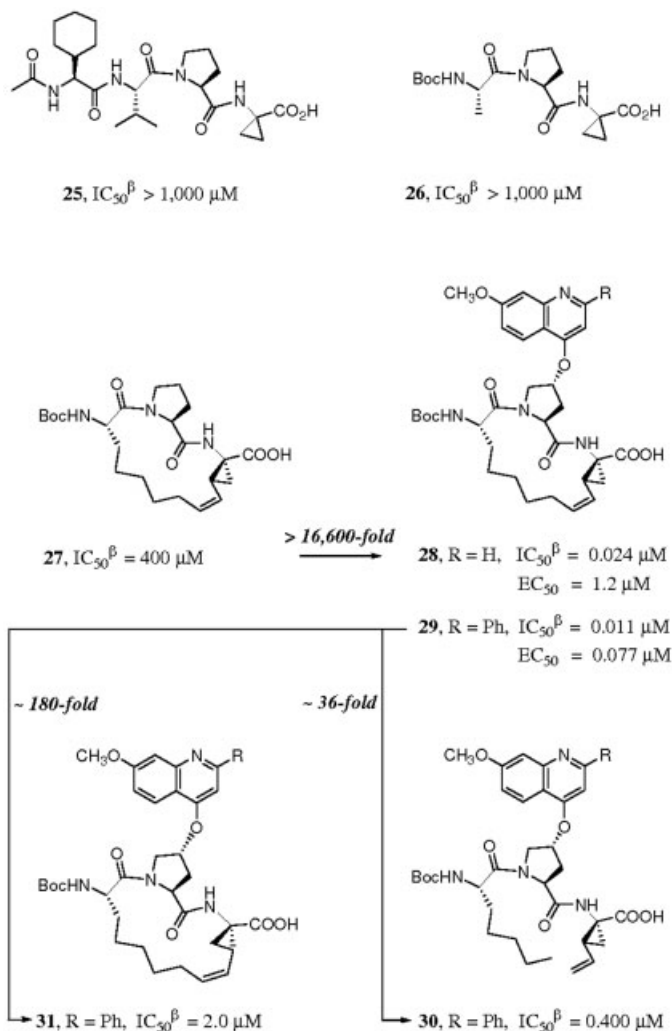
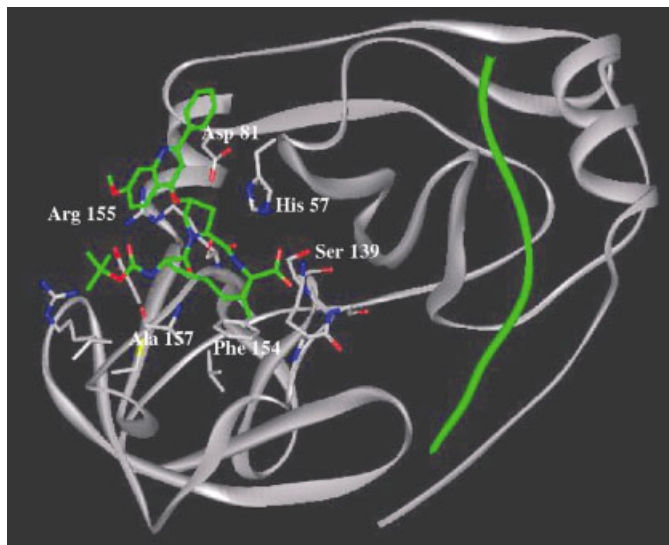


FIGURE 9 Design of macrocyclic inhibitors of the HCV NS3 protease.

### CRYSTALLOGRAPHIC EVIDENCE FOR BINDING OF MACROCYCLIC INHIBITORS IN THE ACTIVE SITE OF THE HCV NS3 PROTEASE

The binding of the macrocyclic inhibitors in the active site of the NS3 protease was confirmed by X-ray crystallography. Previous to our report,<sup>52</sup> crystallographic and NMR data of  $\alpha$ -keto acid inhibitors covalently bound to the NS3 protease had been reported.<sup>58,59</sup> In addition, a crystal structure of an engineered single polypeptide, containing the C-terminal helicase domain and the N-terminal protease covalently linked to the NS4A cofactor, revealed the binding of the C-terminal carboxylic acid moiety of the helicase to the active site of the protease (Figure 2a).<sup>31</sup> The latter report was the only other example of a C-terminal carboxylate bound to the

active site of the NS3/NS4 complex and represented a model of product inhibition for this enzyme. However, the compound 29–NS3 complex (Figure 10) represents the first X-ray structure of a small molecule carboxylic acid inhibitor bound to the active site of the HCV NS3 protease.<sup>52</sup> This structure revealed how the carboxylate group interacts with the active site and provided additional insight into the mechanism of product inhibition observed with natural substrates of the HCV NS3 protease. The heteroatom–heteroatom distances suggested that one of the carboxylate oxygens of the inhibitor binds in the oxyanion hole of the NS3 (NH of G137 and S139), while the other forms a hydrogen bond with the H57 (N $\delta$ ) residue (Figure 10).<sup>52</sup> In addition, the side chain (O $\gamma$ ) of S139 appeared to form weak asymmetric bifurcated H-bonds with both of the carboxylate oxygens of the inhibitor. Formation of canonical hydrogen bonds be-



**FIGURE 10** Structure of inhibitor **29** bound to the HCV NS3/NS4A<sub>peptide</sub> complex as determined by X-ray crystallography (NS3 protease domain is colored in grey, the NS4A<sub>peptide</sub> in green)<sup>51</sup>; the catalytic residues, Asp 81, His 57, and Ser 139, as well as other key residues around the active site, are highlighted in ball-and-stick formation (oxygen atoms indicated in red, nitrogen atoms in blue, and sulfur in yellow).

tween the inhibitor's amide moieties and the NS3 residues R155 and A157 were also observed. The inhibitor's aliphatic linker (between P1 and P3) was clearly visible in the electron density, indicating that it was conformationally fixed within the S1–S3 pocket. The NS3 residue V132 appeared to be within van der Waals distance of this linker and may be contributing to the overall binding energy in the inhibitor–enzyme complex (Figure 10).<sup>52</sup> Furthermore, inhibitor-induced conformational changes of the R155 side chain led to the formation of an interaction between the methoxy group of the P2 quinoline and the guanidinium ion of R155 (Figure 10); the latter observation provided validation for the approach and tools used in the early phases of this drug discovery program, leading to the optimization of the dipole/quadrupole and  $\pi$ -stacking interactions of the tetrapeptide ligands with the NS3 protease.<sup>49</sup> In addition, the macrocyclic inhibitor **29**–NS3 crystal structure provided proof for the molecular basis of interactions between a potent and selective *drug-like* inhibitor and the active site of the NS3 protease.

## OPTIMIZATION OF THE BIOPHARMACEUTICAL PROPERTIES

Preliminary pharmacokinetic studies on the early macrocyclic inhibitors were encouraging, as these compounds were found to be metabolically stable and

orally bioavailable in rats.<sup>52</sup> However, in the absence of a reference drug substance with proven clinical efficacy in HCV- infected patients, it was impossible to predict the potential clinical value of these compounds. Nonetheless, analogs with good pharmacokinetic properties were expected to have a good chance of demonstrating antiviral efficacy in humans. Based on SAR studies, it was observed that the 2-phenyl substituent of the quinoline moiety was particularly amenable to optimization for both cell-based potency and oral absorption. Replacement of the phenyl ring with various heterocyclic rings led to the discovery of highly potent and selective inhibitors of the HCV NS3 protease. Examples are shown in Figure 11 and others have been recently reported.<sup>60</sup> Although the *in vitro* enzymatic potency of these analogs varied very modestly, their cell-based potency was modulated significantly (Figure 11). Modest improvement was also observed in both the enzymatic and cell-based potency when the *t*-butyl carbamate capping group of P3 was replaced by the chemically more stable cyclopentyl carbamate. However, the combined subtle structural modifications were found to have a profound effect on the pharmacokinetic properties of the compounds. For example, administration of inhibitor **29** to rats, at an oral dose of 25 mg/kg and an intravenous dose of 5 mg/kg, resulted in almost undetectable levels of the compound in the plasma ( $C_{\max}$  of 0.2  $\mu\text{M}$ ) and an oral bioavailability of only 2%. In contrast, administration of compound **2** (*BILN 2061*), at an

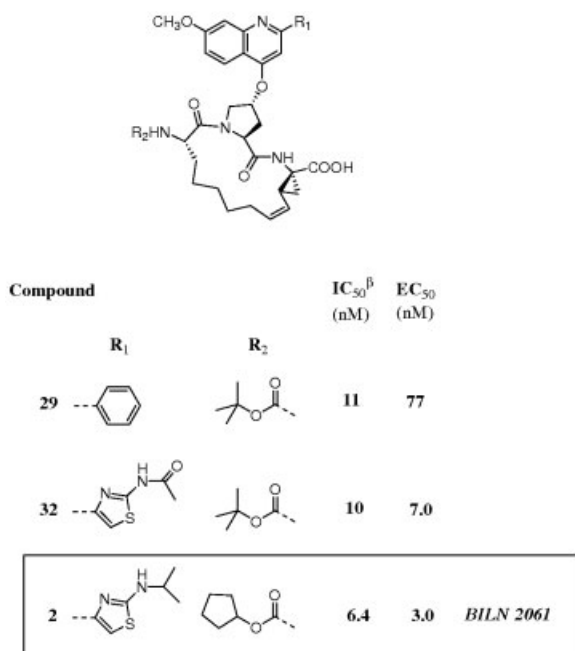


FIGURE 11 Optimization of pharmacokinetic properties.

oral dose of 20 mg/kg and an intravenous dose of 5 mg/kg, resulted in a maximum plasma concentration of 2.5  $\mu\text{M}$ , an area under the plasma concentration–time curve (AUC) of 12.5  $\mu\text{M} \cdot \text{h}$  and an oral bioavailability of 42%. Furthermore, **BILN 2061** had a similar pharmacokinetic profile in animals of higher species.

## CONCLUDING PERSPECTIVES—FROM THE BENCH TO THE CLINIC

Understanding the structure–activity relationship between a chemical probe and its biological target is one of the most challenging tasks in medicinal chemistry. This is primarily because even a minor structural modification of a compound may lead to the introduction of a large number of variable factors that cannot be easily identified or quantified. Compounding these problems, peptidomimetic lead structures are generally plagued with poor biopharmaceutical properties, including poor cell membrane permeability, poor oral absorption, short plasma half-life, and high clearance rates.<sup>61</sup> Nonetheless, in our quest for an inhibitor of the HCV NS3 serine protease, we undertook the challenge of designing a novel class of peptidomimetics that mimic the  $\beta$ -strand conformation of the NS3 protease substrates. These compounds were the first HCV NS3 protease inhibitors reported that could inhibit HCV RNA replication in the cell-based replicon

assay, in addition to being orally absorbed and stable to metabolic breakdown. In addition, the favorable pharmacokinetics observed in several animal species with one such compound, **BILN 2061** (**2**), provided optimism for its further evaluation in humans.<sup>19</sup> When this macrocyclic inhibitor was administered orally to patients infected with HCV genotype 1, for a period of two days, an unprecedented decline in plasma viral load of up to 3 logs was observed. This demonstration of in vivo antiviral activity represents the first proof-of-concept in humans for HCV NS3 protease inhibitors. Furthermore, the clinical efficacy of **BILN 2061** has provided validation for the tools currently used for advancing compounds from predevelopment to the clinic in hepatitis C research programs worldwide.

## REFERENCES

- Choo, Q.-L.; Kuo, G.; Weiner, A. J.; Overby, L. R.; Bradley, D. W.; Houghton, M. *Science* 1989, 244, 359–362.
- Wasley, A.; Alter, M. J. *Sem Liver Dis* 2000, 20, 1–16.
- Berenger, M.; Wright, T. L. *Proc Assoc Am Phys* 1998, 110, 98–112.
- Forns, X.; Bukh, J.; Purcell, R. H. *J Hepatol* 2002, 37, 684–695.
- Hadziyannis, S. J.; Papatheodoridis, G. V. *Expert Opin Pharmacother* 2003, 4, 541–551.
- Chander, G.; Sulkowski, M. S.; Jenckes, M. W.; Torbenson, M. S.; Herlong, F.; Bass, E. B.; Gebo, K. A. *Hepatology* 2002, 36, S135–144.
- Robertson, B.; Myers, G.; Howard, C.; Brettin, T.; Bukh, J.; Gaschen, B.; Gojobori, T.; Maertens, G.; Mizokami, M.; Nainan, O.; Netesov, S.; Nishioka, K.; Shin-i, T.; Simmonds, P.; Smith, D.; Stuyver, L.; Weiner, A. *Arch Virol* 1998, 143, 2493–2503.
- Hijikata, M.; Kato, N.; Ootsuyama, Y.; Nakagawa, M.; Shimotohno, K. *Proc Natl Acad Sci USA* 1991, 88, 5547–5551.
- Grakoui, A.; Wychowski, C.; Lin, C.; Feinstone, S. M.; Rice, C. M. *J Virol* 1993, 67, 1385–1395.
- Kolykhalov, A. A.; Mihalik, K.; Feinstone, S. M.; Rice, C. M. *J Virol* 2000, 74, 2046–2051.
- Walker, M. P.; Yao, N.; Hong, Z. *Expert Opin Invest Drugs* 2003, 12, 1269–1280.
- Tan, S.-L.; Pause, A.; Shi, Y.; Sonenberg, N. *Nature Rev* 2003, 1, 867–881.
- De Francesco, R.; Tomei, L.; Altamura, S.; Summa, V.; Migliaccio, G. *Antiviral Res* 2003, 58, 1–16.
- Lohmann, V.; Körner, F.; Koch, J.-O.; Herian, U.; Theilmann, L.; Bartenschlager, R. *Science* 1999, 285, 110–113.
- Bartenschlager, R.; Kaul, A.; Sparacio, S. *Antiviral Res* 2003, 60, 91–102.
- Landford, R. E.; Bigger, C.; Bassett, S.; Klimpel, C. *ILAR J* 2001, 42, 117–126.

17. Grakoui, A.; Hanson, H. L.; Rice, C. M. *Hepatology* 2001, 33, 489–495.
18. Mercer, D. F.; Schiller, D. E.; Elliott, J. F.; Douglas, D. N.; Hao, C.; Rinfret, A.; Addison, W. R.; Fisher, K. P.; Churchill, T. A.; Lakey, J. R. T.; Tyrrell, D. L. J.; Kneteman, N. M. *Nature Med* 2001, 7, 927–933.
19. Lamarre, D.; Anderson, P. C.; Bailey, M.; Beaulieu, P.; Bolger, G.; Bonneau, P.; Bós, M.; Cameron, D.; Cartier, M.; Cordingley, M. G.; Faucher, A.-M.; Goudreau, N.; Kawai, S. H.; Kukolj, G.; Lagacé, L.; LaPlante, S. R.; Narjes, H.; Poupert, M.-A.; Rancourt, J.; Sentjens, R. E.; St George, R.; Simoneau, B.; Steinmann, G.; Thibeault, D.; Tsantrizos, Y. S.; Weldon, S. M.; Yong, C.-L.; Llinàs-Brunet, M. *Nature* 2003, 426, 186–189.
20. Hinrichsen, H.; Benhamou, Y.; Reiser, M.; Sentjens, R.; Wedemeyer, H.; Calleja, J. L.; Fornis, X.; Croenlein, J.; Nehmiz, G.; Steinmann, G. *Hepatology* 2002, 36(4, Part 2), 379A (2002 AASLD Meeting, Abstract 866).
21. Rice, C. M. *Nature* 2003, 426, 129–130.
22. Santolini, E.; Migliaccio, G.; La Monica, N. *J Virol* 1994, 68, 3631–3641.
23. Lin, C.; Lindenbach, B. D.; Pragai, B. M.; McCourt, D. W.; Rice, C. M. *J Virol* 1994, 68, 5063–5073.
24. Houghton, M.; Weiner, A.; Han, J.; Kuo, G.; Choo, Q. L. *Hepatology* 1991, 14, 381–388.
25. Hijikata, M.; Mizushima, H.; Akagi, T.; Mori, S.; Kakiuchi, N.; Kato, N.; Tanaka, K.; Kimura, K.; Shimotohno, K. *J Virol* 1993, 67, 4665–4675.
26. Mizushima, H.; Hijikata, M.; Tanji, Y.; Kimura, K.; Shimotohno, K. *J Virol* 1994, 68, 2731–2734.
27. De Francesco, R.; Steinkühler, C. *Curr Top Microbiol Immunol* 2000, 242, 149–169.
28. Steinkühler, C.; Koch, U.; Narjes, F.; Matassa, V. G. *Curr Med Chem* 2001, 8, 919–932.
29. Kim, D.W.; Gwack, Y.; Han, J. H.; Choe, J. *Biochem Biophys Res Commun* 1995, 215, 160–166.
30. Yao, N.; Reichert, P.; Taremi, S. S.; Prosise, W. W.; Weber, P. C. *Structure Fold Design* 1999, 7, 1353–1363.
31. Morgenstern, K. A.; Landro, J. A.; Hsiao, K.; Lin, C.; Gu, Y.; Su, M. S.-S.; Thomson, J. A. *J Virol* 1997, 71, 3767–3775.
32. Gallinari, P.; Brennan, D.; Nardi, C.; Brunetti, M.; Tomei, L.; Steinkühler, C.; De Francesco, R. *J Virol* 1998, 72, 6758–6769.
33. Review: Bartenschlager, R. *J Viral Hepat* 1999, 6, 165–181.
34. Love, R. A.; Parge, H. E.; Wickersham, J. A.; Hostomsky, Z.; Habuka, N.; Moomaw, E. W.; Adachi, T.; Hostomska, Z. *Cell* 1996, 87, 331–342.
35. Yan, Y.; Li, Y.; Munshi, S.; Sardana, V.; Cole, J. L.; Sardana, M.; Steinkühler, C.; Tomei, L.; De Francesco, R.; Kuo, L. C.; Chen, Z. *Protein Sci* 1998, 7, 837–847.
36. Kim, J. L.; Morgenstern, K. A.; Lin, C.; Fox, T.; Dwyer, M. D.; Landro, J. A.; Chambers, S. P.; Markland, W.; Lepre, C. A.; O'Malley, E. T.; Harbeson, S. L.; Rice, C. M.; Murcko, M. A.; Caron, P. R.; Thomson, J. A. *Cell* 1996, 87, 343–355.
37. Llinàs-Brunet, M.; Bailey, M.; Fazal, G.; Goulet, S.; Halmos, T.; LaPlante, S.; Maurice, R.; Poirier, M.; Poupert, M.-A.; Thibeault, D.; Wernic, D.; Lamarre, D. *Bioorg Med Chem Lett* 1998, 8, 1713–1718.
38. Ingallinella, P.; Altamura, S.; Bianchi, E.; Taliani, M.; Ingenito, R.; Cortese, R.; De Francesco, R.; Steinkühler, C.; Pessi, A. *Biochemistry* 1998, 37, 8906–8914.
39. Protease subsite nomenclature: Schechter, I.; Berger, A. *Biochem Biophys Res Commun* 1967, 27, 157–160.
40. Llinàs-Brunet, M.; Bailey, M.; Déziel, R.; Fazal, G.; Gorys, V.; Goulet, S.; Halmos, T.; Maurice, R.; Poirier, M.; Poupert, M.-A.; Rancourt, J.; Thibeault, D.; Wernic, D.; Lamarre, D. *Bioorg Med Chem Lett* 1998, 8, 2719–2724.
41. Llinàs-Brunet, M.; Bailey, M.; Fazal, G.; Ghio, E.; Gorys, V.; Goulet, S.; Halmos, T.; Maurice, R.; Poirier, M.; Poupert, M.-A.; Rancourt, J.; Thibeault, D.; Wernic, D.; Lamarre, D. *Bioorg Med Chem Lett* 2000, 10, 2267–2270.
42. Thibeault, D.; Bousquet, C.; Gingras, R.; Lagacé, L.; Maurice, R.; White, P. W.; Lamarre, D. *J Virol*, in press.
43. LaPlante, S. R.; Cameron, D. R.; Aubry, N.; Lefebvre, S.; Kukolj, G.; Maurice, R.; Thibeault, D.; Lamarre, D.; Llinàs-Brunet, M. *J Biol Chem* 1999, 274, 18618–18624.
44. LaPlante, S. R.; Aubry, N.; Déziel, R.; Ni, F.; Xu, P. *J Am Chem Soc* 2000, 122, 12530–12535.
45. Cicero, D. O.; Barbato, G.; Koch, U.; Ingallinella, P.; Bianchi, E.; Nardi, M. C.; Steinkühler, C.; Cortese, R.; Matassa, V.; De Francesco, R.; Pessi, A.; Bazzo, R. *J Mol Biol* 1999, 289, 385–396.
46. Koch, U.; Biasiol, G.; Brunetti, M.; Fattoti, D.; Palaoro, M.; Steinkühler, C. *Biochemistry* 2001, 40, 631–640.
47. Nam, N.-H.; Sardari, S.; Parang, K. *J Combinat Chem* 2003, 5, 497–546.
48. Miyaura, N.; Suzuki, A. *Chem Rev* 1995, 95, 2457–2483.
49. Poupert, M.-A.; Cameron, D. R.; Chabot, C.; Ghio, E.; Goudreau, N.; Goulet, S.; Poirier, M.; Tsantrizos, Y. S. *J Org Chem* 2001, 66, 4743–4751.
50. Goudreau, N.; Cameron, D. R.; Bonneau, P.; Gorys, V.; Plouffe, C.; Poirier, M.; Lamarre, D.; Llinàs-Brunet, M. *J Med Chem* 2004, 47, 123–132.
51. Dougherty, D. A. *Science* 1996, 271, 163–168.
52. Tsantrizos, Y. S.; Bolger, G.; Bonneau, P.; Cameron, D. R.; Goudreau, N.; Kukolj, G.; LaPlante, S. R.; Llinàs-Brunet, M.; Nar, H.; Lamarre, D. *Angew Chem Int Ed* 2003, 42, 1356–1360.
53. Rancourt, J.; Cameron, D. R.; Gorys, V.; Lamarre, D.; Poirier, M.; Thibeault, D.; Llinàs-Brunet, M. *J Med Chem* 2004, 47, 2511–2522.
54. LaPlante, S. R.; Aubry, N.; Bonneau, P. R.; Kukolj, G.; Lamarre, D.; Lefebvre, S.; Li, H.; Llinàs-Brunet, M.;

- Plouffe, C.; Cameron, D. R. *Bioorg Med Chem Lett* 2000, 10, 2271–2274.
55. Goudreau, N.; Brochu, C.; Cameron, D. R.; Duceppe, J.-S.; Faucher, A.-M.; Ferland, J.-M.; Grand-Maitre, C.; Poirier, M.; Simoneau, B.; Tsantrizos, Y. S. *J Org Chem* 2004, Web release August 18, 2004.
56. Khan, A. R.; Parrish, J. C.; Fraser, M. E.; Smith, W. W.; Bartlett, P. A.; James, M. N. G. *Biochemistry* 1998, 37, 16839–16845.
57. Tsantrizos, Y. S.; et al., unpublished data.
58. Barbato, G.; Cicero, D. O.; Cordier, F.; Narjes, F.; Gerlach, B.; Sambucini, S.; Grzesiek, S.; Matassa, V. G.; De Francesco, R.; Bazzo, R. *EMBO J* 2000, 19, 1195–1206.
59. Di Marco, S.; Rizzi, M.; Volpari, C.; Walsh, M. A.; Narjes, F.; Colarusso, S.; De Francesco, R.; Matassa, V. G.; Sollazzo, M. *J Biol Chem* 2000, 275, 7152–7157.
60. Llinàs-Brunet, M.; Bailey, M. D.; Bolger, G.; Brochu, C.; Faucher, A.-M.; Ferland, J. M.; Garneau, M.; Ghio, E.; Gorys, V.; Grand-Maitre, C.; Halmos, T.; Lapeyre-Paquette, N.; Liard, F.; Poirier, M.; Rhéaume, M.; Tsantrizos, Y. S.; Lamarre, D. *J Med Chem* 2004, 47, 1605–1608.
61. Denissen, J. F.; Grabowski, B. A.; Johnson, M. K.; Buko, A. M.; Kempf, D. J.; Thomas, S. B.; Surber, B. W. *Drug Metab Dispos* 1995, 23, 185–189.